Journal of Catalysis 369 (2019) 296–301

Contents lists available at ScienceDirect

Journal of Catalysis

journal homepage: www.elsevier.com/locate/jcat

Metal-free silicon boride catalyst for oxidative dehydrogenation of light alkanes to olefins with high selectivity and stability

Bing Yan, Wen-Cui Li, An-Hui Lu *

School of Chemical Engineering, State Key Laboratory of Fine Chemicals, Dalian University of Technology, Dalian 116024, PR China

ARTICLE INFO

Article history:
Received 26 August 2018
Revised 25 October 2018
Accepted 11 November 2018
Available online 28 November 2018

Keywords:
Oxidative dehydrogenation
Light alkanes
Silicon boride
Metal-free catalyst

ABSTRACT

Due to the free coking and no equilibrium limitation in alkanes conversion, the oxidative dehydrogenation of light alkanes to olefins offers an attractive route, but encounters the difficulty in selectivity control for olefins because of the over-oxidation reactions that produce a substantial amount of CO_2. Here we report silicon boride exhibiting good oxidation resistance property at high temperature, as a metal-free catalyst efficiently catalyzed dehydrogenation of light alkanes to olefins with a high selectivity at a given reaction conditions. The stability was evidenced by the operation of a 100-h test with steady conversion and product selectivity. When the conversion of ethane, propane and isobutane reached 18.8%, 19.1% and 6.0%, the selectivity of olefins were up to 98.0%, 94.4% and 96.4%, respectively. This work experimentally supports that the catalytic origin of the boron species from the metal-free catalyst initiate the oxidative dehydrogenation of light alkanes.

1. Introduction

The heterogeneous oxidative dehydrogenation (ODH) of light alkanes (C_2–C_4) featured with free coking and no thermodynamic restriction is an attractive process to direct dehydrogenation, and usually catalysed by transition metal oxides and alkaline-earth metal oxychlorides [1–7]. Nevertheless, the uncontrollable over-oxidation of olefins caused the formation of significant amounts of CO_2 (10–60%) [8–12], which made the metal oxides or oxychlorides catalysed ODH process is still far away in prospect of industrialization.

The recent discovery that antioxidant and chemically inert hexagonal boron nitride (*h*-BN) is extremely active for ODH process of ethane and propane opens up a new research direction in selective cleavage of C—H bond of alkanes by the metal-free catalyst [13–15]. It consequently expands the fundamental understanding of the industrially important ODH process. The catalyst *h*-BN can convert propane to propylene with a selectivity reaching ~80%, more than 90% for both propylene and ethylene, with negligible CO_2 formation (0.5%) at a given propane conversion of 20.6% [14]. Hermans and co-workers proposed that B—O—O—N [13], later on boron oxygen species [16] were responsible for high activity and olefins selectivity that were influenced by electronic interactions between active sites and adjacent structures. Our spectroscopic investigation suggested that the B—OH could be the active sites which selectively broke the C—H bond but simultaneously shut off the pathway of propylene overoxidation towards CO_2 [14,17]. In the following up study, Su et al. proposed that and the B—O(H) formed at the edges of *h*-BN were the active sites for ethane ODH reaction. Recently [18], we showed that boron nitride can also oxidize methane to valuable products [19]. Moreover, Xie and coworkers demonstrated that carbon-doped BN catalyst showed good activity in ODH of ethylbenzene to styrene [20]. Anyhow, people in different groups identified with the idea that the boron species could be truly indispensable element for high ODH activity.

Silicon boride ($SiB_{3\text{-}6}$), a metal-free material enriching in boron sites, exhibits good oxidation resistance property at high temperature and could be as a potential catalyst for ODH of light alkanes. Study on the metal-free silicon boride may make a better understanding on the catalytic origin of the boron species, and further initiate the exploration of other new boron-based catalysts. Herein, we prepared an oxygenic groups functionalised silicon boride (main phase is SiB_6, Fig. S1) for ODH of light alkanes. The functionalised silicon boride showed high ODH activity for light alkanes; more importantly, the antioxidant ability of silicon boride ensured the catalytic stability.

2. Experimental

2.1. Catalyst preparation

Silicon boride was purchased from Shanghai Lantian nanomaterial Co., Ltd.. Before using, the silicon boride was first impregnated

* Corresponding author.
E-mail address: anhuilu@dlut.edu.cn (A.-H. Lu).

https://doi.org/10.1016/j.jcat.2018.11.014
0021-9517/

with 4 M NaOH aqueous solution at 50 °C for 24 h, afterwards, the sample was washed by aqueous ammonia, followed extensive washing with ultrapure water, and then dried at 100 °C in air.

2.2. Catalytic evaluation

Catalytic reactions were performed in a packed-bed quartz microreactor (I.D. = 6 mm). The reaction mixture was alkanes/oxygen/nitrogen with a molar ratio of 1/1/4 for ethane, 1/1.5/3.5 for propane and 1/0.5/4.5 for isobutane at atmospheric pressure. The flow rate was fixed at 48 mL min^{-1}, and the reaction temperature was varied in the range of 450–595 °C. SiC (β phase, 0.25 mm-0.43 mm) was used as the control sample for blank test and the results were showed in Table S1. Reactants and products were analyzed by an online gas chromatograph (Techcomp, GC 7900). A GDX-102 and 5A molecular sieve column, connected to a TCD and a Plot Al_2O_3/S column connected to an FID were used to analyze the O_2, N_2, i-C_4H_{10}, i-C_4H_8, C_3H_8, C_3H_6, C_2H_6, C_2H_4, CH_4, CO, and CO_2.

Conversion was defined as the number of moles of carbon converted divided by the number of moles of carbon present in the feed. Selectivity was defined as the number of moles of carbon in the product divided by the number of moles of carbon reacted. The turnover rate (TOR) was calculated based on the hypothesis that per boron atom generates one B—OH in B_2O_3 and B_xO_y species. The quantity of BO species was calculated from the results of XPS and mass change of catalysts (before and after reaction) due to the oxidation of catalyst surfaces. The number of active sites were 8×10^{-3} - $mol_{BOHsite}$ g_{cat}^{-1}. The carbon balance was checked by comparing the number of moles of carbon in the outlet stream to the number of moles of carbon in the feed. Under our typical evaluating conditions, the carbon balance was higher than 95%. To account for the volume expansion in the reaction, nitrogen was used as the internal standard.

In kinetic analysis, reaction rates were measured in a packed-bed single-pass flow microreactor with plug-flow hydrodynamics. Catalyst samples weighing were 0.1–0.2 mg (0.25–0.43 mm). Experimental data of alkanes and oxygen conversion at different temperature levels were used to obtain the apparent activation energy. Reaction orders of alkanes and oxygen were obtained by measuring the effect of reactant partial pressure on reaction rates. The catalytic reactions were not affected by mass or heat transport limitations (Fig. S2).

2.3. Catalyst characterization

XPS analysis was performed on an Omicron Sphera II hemispherical electron energy analyzer with an in-situ reaction cell attached to the instrument. Monochromatic ALK X-ray source (1486.6 eV, anode operating at 15 kV and 300 W) was used as incident radiation. Before the measurements, all the samples were treated in situ at 500 °C for 1 h under an Ar stream (32 mL min^{-1}) and then moved to the measured chamber under vacuum conditions.

Nitrogen sorption isotherms were measured with a Tristar 3000 sorption analyzer (Micromeritics). Brunauer–Emmett–Teller (BET) method was used to calculate the specific surface areas.

Transmission electron microscopy (TEM) images (Fig. S3) were recorded on a FEI TECNAI F30 microscope, operating at an accelerating voltage of 300 kV. Scanning electron microscope-Energy Dispersive Spectrometer (SEM-EDS) investigations were carried out with a FEI Nova NanoSEM 450 instrument.

In situ X-ray powder diffraction (XRD) measurements were operated on a PANalytical X'Pert3 Powder diffractometer using Cu Kα radiation (λ = 0.15406 nm). The tube voltage was 40 kV, and the current was 40 mA. The 150 mg catalyst was loaded into the reactor chamber and heated in nitrogen at a rate of 10 °C/min to 535 °C under a flow of N_2. Subsequently, the gas flow was switched to O_2/N_2 or $C_3H_8/O_2/N_2$ to determine the change occurred in different environment for catalyst. The flow rate was fixed as 48 mL/min.

In situ DRIFT spectra were recorded under reaction condition on a Nicolet 6700 FTIR spectrometer equipped with mercury cadmium telluride (MCT) detector. The 20 mg silicon boride catalyst was loaded into the cell with a CaF_2 window. Spectra were averaged over 256 scans in the range 400–4000 cm^{-1} with a 2 cm^{-1} resolution. The gas composition at the reactor outlet during was controlled by online mass spectrometry (MS, Pfeiffer, OminStar™). The *m*/*z* of 41 was used to analyze C_3H_6. The contribution of C_3H_8 for the *m*/*z* signal of 41 was deducted.

Isotope-labeling experiments were performed in a packed-bed single-pass flow microreactor. The chemical and isotopic compositions of the reactor effluent were measured by online mass spectrometry. In the deuterium-labeling studies, the silicon boride catalyst was initially treated at 535 °C under N_2 (50 mL min^{-1}) for 2 h, and then a 12 h H/D exchange process on the catalyst surface was accomplished by passing a N_2 feed (30 mL min^{-1}) through a water saturator held at 25 °C by a thermostat to produce a 3.5 vol % D_2O/N_2 feed. Heavy water (D_2O, Cambridge Isotope Lab., 99.9%) was not further purified. Subsequently, the catalyst was purged with the N_2 (50 mL min^{-1}) for 3 h to remove the excess D_2O. A mixture of the two (800 mL each time) was then directly pulsed into the catalyst using N_2 (50 mL min^{-1}) as the carrier gas. The following mass-to-charge (*m*/*z*) signals were analyzed: 29 (C_3H_8), 41 (C_3H_6, C_3H_8), 18 (H_2O), 19 (HDO), and 20 (D_2O).

3. Results and discussion

3.1. Catalytic performance of silicon boride

Before using, the silicon boride was activated by feed gas ($C_3H_8/O_2/N_2$) at 535 °C for 3 h (possible impurity elements were showed in Table S2). The activity of silicon boride catalyst in ODH of light alkanes including ethane, propane and isobutane was showed in Fig. 1. The first example is ODH of ethane. The TOR of ethane approached 1.3×10^{-3} mol s^{-1} mol_{site}^{-1} (Table 1) at 575 °C and the ethylene selectivity reached 95.8% with CO_x (4.2%) as byproduct. The superior catalytic selectivity is better than those of carbon-based catalysts [21] and many metal oxide catalysts [22] (Fig. S4). In another case of ODH of propane, the TOR was 9×10^{-4} mol s^{-1} mol_{site}^{-1} at 535 °C and the selectivity of propylene was 82.2%. Taking the valuable product ethylene into account,

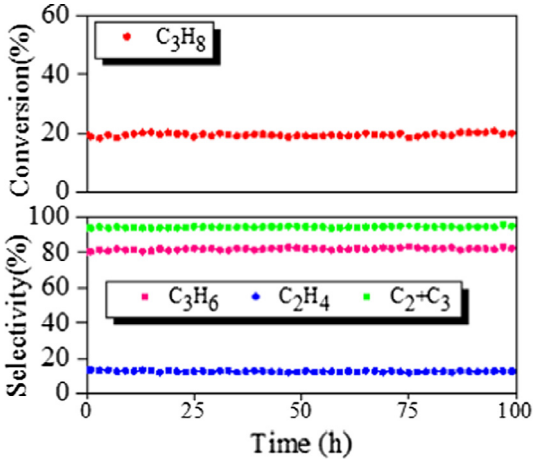

Fig. 1. Long-term stability test of propane at 535 °C; gas feed, 16.6 vol% C_3H_8 (8 mL/min), 25.2 vol% O_2, and N_2 balance.

Table.1
Catalytic performance alkanes turnover rate (TOR) and olefins selectivity.

Reactants[a]	Temperature (°C)	Conversion (%)	TOR ($\times 10^{-3}$ mol s^{-1} $mol^{-1}_{BOHsite}$)	Selectivity (%)			
				i-C_4H_8	C_3H_6	C_2H_4	CO_x
C_2H_6	585	45.9	2.2	–	–	89.2	10.8
	575	28.2	1.3	–	–	95.8	4.2
C_3H_8	545	31.1	1.5	–	72.1	16.6	10.2
	535	19.2	0.9	–	82.2	12.2	5.2
i-C_4H_{10}	520	15.6	0.7	62.5	28.4	–	3.0
	490	6.0	0.3	77.1	19.3	–	1.0

[a] The catalytic activity of silicon boride catalyst in ODH of (a) ethane ($C_2H_6/O_2/N_2$ = 1:1:4), (b) propane ($C_3H_8/O_2/N_2$ = 1:1.5:3.5), (c) isobutane (i-$C_4H_{10}/O_2/N_2$ = 1:0.5:4.5) at different temperatures; catalyst weight, 100 mg; total flow rate of 48 mL/min.

the selectivity of light olefins including ethylene and propylene reached 94.4%, superior to that over most metal oxide catalysts [23,8], carbon materials [24,25]. In the case of ODH of isobutane, the TOR was 3×10^{-4} mol s^{-1} mol^{-1}_{site} at 490 °C and the 77.1% selectivity of isobutene (96.4% selectivity of olefins) was observed. The selectivity of olefins is better than most of other metal-based and carbon-based catalysts [26,27] (Fig. S4). The catalytic selectivity of silicon boride catalyst was also higher than most of other boron-containing catalysts [16,18]. The difference of selectivity between silicon boride with other boron-containing catalysts maybe resulted from the different subsurface structure [16]. In addition, light olefins productivities reported on most metal oxide catalysts and boron-based catalysts were lower than 1 $g_{olefins}$ g_{cat}^{-1} h^{-1}, unattractive for commercial application [12,16]. In our case, the light olefins productivity was 1.2–2.6 $g_{olefins}$ g_{cat}^{-1} h^{-1}, demonstrating a good activity of the silicon boride catalyst for catalytic production of light olefins. The stability of the silicon boride catalyst in the ODH of propane to propylene was evidenced by the operation of a 100-h test at 535 °C. No significant variations in the conversion and product selectivity occurred (Fig. 1). It needed to note that the catalytic activity of silicon boride was increasing over time during the activation process (Fig. S5), as we observed in *h*-BN catalytic system[14]. More interestingly, the propane conversion rate of the catalyst activated in oxygen atmosphere (535 °C, 3 h; the catalyst was defined as SiB-O_2) was much lower than that activated under reaction conditions (Table S3).

3.2. The origin of catalytic activity

An introduction period was observed on silicon boride catalysts which was also found in *h*-BN catalyzing ODH reactions [17,28]. To better understand the activation and reaction process, XRD measurement was performed to trace the structure evolution of the silicon boride catalyst under different conditions, including heated to 535 °C, activated in oxygen or reaction atmosphere and then cooled to room temperature (Fig. 2a). When silicon boride catalyst was activated in the reaction atmosphere and then cooled down to room temperature, the characteristic peaks (marked by blue asterisks) associated with B_2O_3 phase were observed, which implied that the origin of the unanticipated catalytic activity might be attributed to the existence of B_2O_3 species. It must be pointed out that the B_2O_3 signal cannot be detected at 535 °C for the low melting point of B_2O_3. In contrast, the bulk phase structure of silicon boride remained unchanged in the oxygen atmosphere at any stages except for slight peak shifts due to a change in lattice parameters resulted from the thermal expansion, implying that the oxyfunctionalization of catalyst was facilitated under ODH reaction conditions. After being subjected to ODH reaction, the catalyst retained the bulk structure of silicon boride (Fig. S1), suggesting that the oxyfunctionalization may only occur on the surface of catalyst.

To further identify the active sites, the structure evolution of the silicon boride catalyst before and after activation was character-

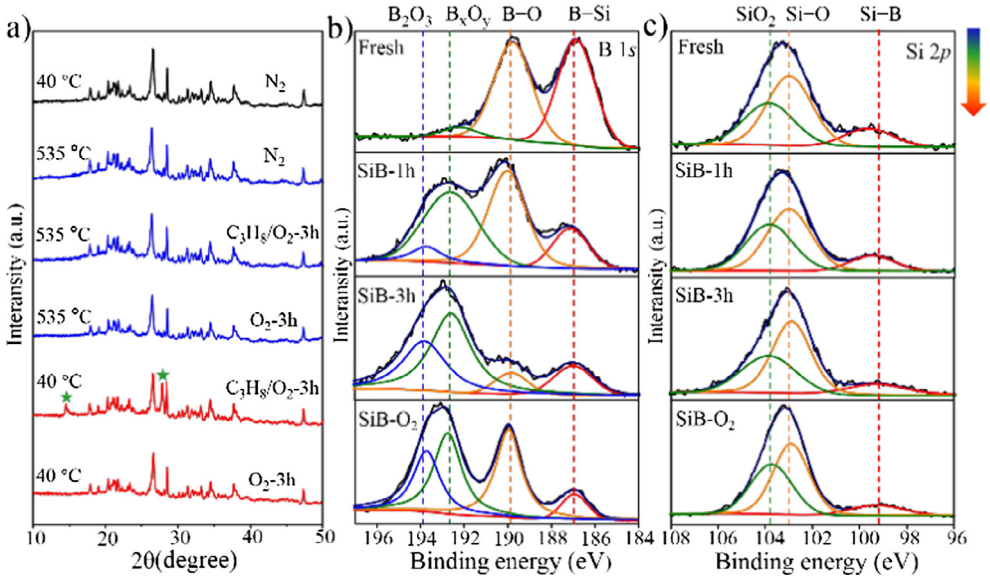

Fig. 2. (a) XRD patterns of catalyst at 40 °C (blank line), heated to 535 °C (blue lines), activated in reaction atmosphere or in oxygen at 535 °C and both cooled to 40 °C (red lines); (b) B 1s, (c) Si 2p XPS spectra for fresh catalyst, exposing to the ODH of propane reaction after 1 h, 3 h and oxygen atmosphere (3 h).

ized by X-ray photoelectron spectroscopy (XPS) analysis. The surface concentrations of boron, silicon and oxygen of a fresh catalyst were 37.7%, 20.5% and 41.8%, respectively (Table S4). In the B 1s XPS spectrum of the fresh catalyst, the percentages of B—Si bond (187.0 eV) and B—O bond (189.8 eV) were 49.4% and 46.6%, while the suboxide (B_xO_y, $y/x < 1.5$, 192.6 eV) species [29] contributed the rest 4.0% (Fig. 2b). The Si 2p signal can be deconvoluted into three peaks centered at 99.4 eV, 102.8 eV and 103.3 eV, corresponding to Si—B bonds, Si—O bonds and the silica (SiO_2, 103.8 eV) (Fig. 2c). Upon exposure to the ODH of propane reaction (535 °C), the surface oxygen concentrations increased to 50.4% after 1 h (SiB-1h) and 54.8% after 3 h (SiB-3h) (Table S4). Furthermore, a higher binding energy of the B 1s signal located at 193.8 eV was detected for SiB-1h and SiB-3h catalysts, which was assigned to the boron oxide (B_2O_3, Fig. 2b). The specific surface area decreased from 23 $m^2\ g^{-1}$ to 5 $m^2\ g^{-1}$ after 3 h might attribute to the formation of B_2O_3. However, as the catalytic activity increasing during the activation process, the concentrations of boron decreased to 31.8% after 1 h and 30.2% after 3 h, estimated from the B 1s XPS spectrum, suggesting that the catalytic activity was not direct related to boron concentration on the surfaces of the silicon boride. In contrast, the percentages of "BO species" (B_xO_y and B_2O_3) in B 1s XPS spectrum increased to 46.8% after 1 h and 79.7% after 3 h, indicating that the increased catalytic activity might relate to the newly generated "BO species".

After running catalyst for 9 h, the XPS spectra had no obvious changes referring to SiB-3h (Fig. S6), suggesting the surface of silicon boride retained stable after 3 h reactions. This can be explained by the antioxidant ability of silicon boride. In addition, the XPS analysis (Fig. 2b) identified that the oxygen and "BO species" concentrations of the SiB-O_2 catalyst were lower than those of the SiB-3h catalyst. Interestingly, Zhou et al. [28] showed that the *h*-BN activated by C_2H_6 and O_2 presented much higher performance than treated with O_2 or C_2H_6 solely. These phenomena demonstrated that the catalyst could be more effectively oxidized in reaction atmosphere. One of the speculated reasons is the in situ generated water on the catalysts surface can accelerate the oxidation rate of boride [30]. In addition, the presence of alkane may promote molecular oxygen dissociation then produce oxygen radicals [17] and leading to more effective oxidation of catalysts.

We conducted in situ Diffuse Reflectance Infrared Fourier-Transform (DRIFT) spectroscopy coupled with an online mass spectroscopy (MS) for simultaneous monitoring the catalyst and the product of propane ODH, in order to better understand the reaction process (Fig. 3). As the reaction proceeding, the DRIFT difference spectra of the catalyst and the corresponding MS signal of

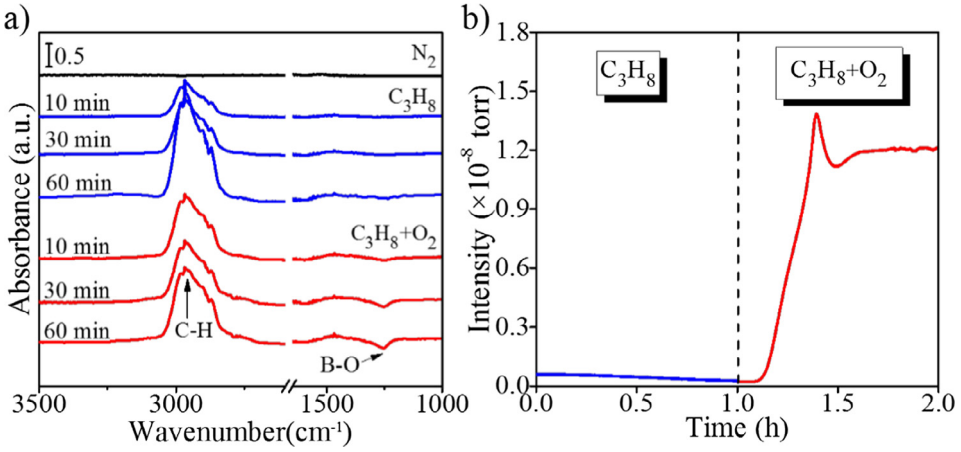

Fig. 3. (a) In situ DRIFT difference spectra and (b) mass spectra of C_3H_6 species at 470 °C under C_3H_8 (blue line) and C_3H_8/O_2 (red line) atmospheres.

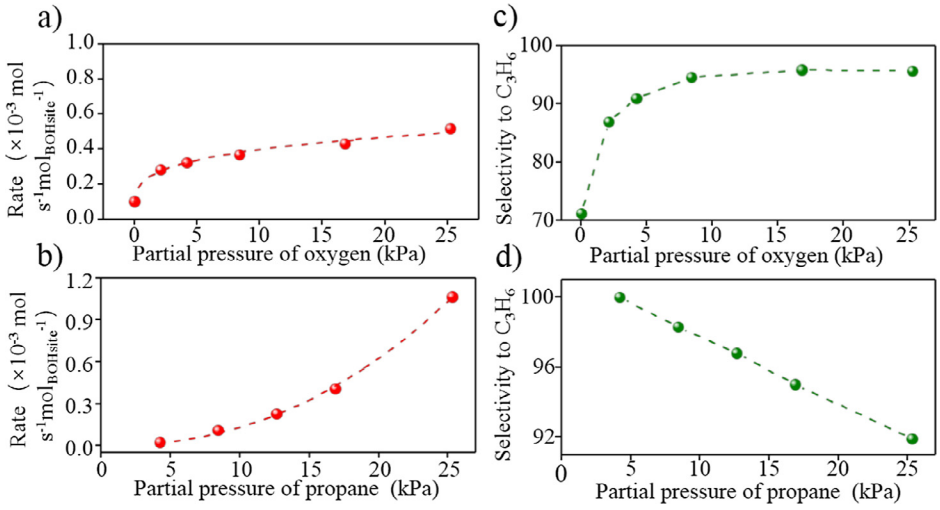

Fig. 4. Effect of partial pressures of oxygen and propane on the converting rate of propane (a, b), and the selectivity to propylene (c, d) in ODH of propane over the silicon boride. Reaction conditions: gas feed, 0–25.2 vol% C_3H_8, 0–25.2 vol% O_2, and N_2 balance; temperature, 510 °C; 0.1 MPa.

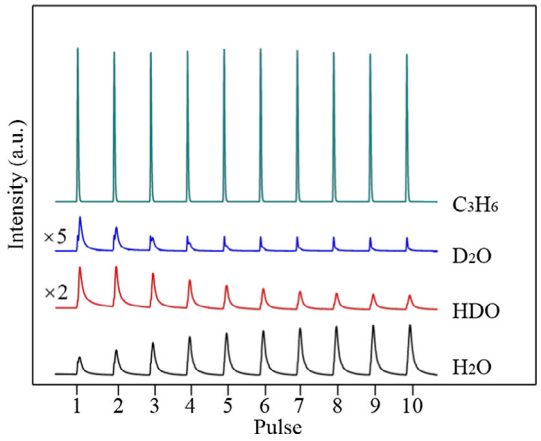

Fig. 5. Mass spectra of C_3H_6, H_2O, HDO, and D_2O species upon pulsing C_3H_8 and O_2 onto the SiB-D catalyst at 535 °C.

propylene were recorded under aerobic or anaerobic conditions by switching the feed gas from N_2 to C_3H_8 and then to C_3H_8/O_2, respectively. Under the C_3H_8 atmosphere, the strong alkyl stretching signal at 2965 cm^{-1} is attributable to the presence of propane gas [31], and no MS signal of propylene was detected (see the blue line in Fig. 3b), which indicates the silicon boride catalyst is unreactive for the dehydrogenation of propane under anaerobic conditions. With the addition of molecular oxygen, the stretching of boron-oxygen [32,33] (B—O) for "BO species" at ~1250 cm^{-1} gradually reduced, accompanied with the formation of propylene (see the red line in Fig. 3b), suggesting that the B—O groups were incorporated into the reaction network. Moreover, when catalyst was just exposed to O_2 atmosphere, the position of the absorption band of silicon boride catalyst remained unchanged (Fig. S8), indicating that the catalyst did not interact with O_2 in the absence of propane.

Huang et al. [18] reported that the B—O sites formed at the edges of *h*-BN were the active sites in the ODH of ethane. Grant et al. [16] found that the high selectivity of propylene in the ODH of propane was related to the formation of BO_x active site at the surfaces of *h*-BN and boron-containing catalysts. Our previous work [12] demonstrated that the B—OH sites initially reacted with molecular oxygen leading to the production of B—O—O—B intermediates and further abstracted the hydrogen atoms from propane, forming C_3H_6 and H_2O in the ODH of propane. Besides, Zhou et al. [28] further proved that the B–OH species can promote the adsorption of O_2 through adsorption microcalorimetric experiments. In this work, the results in Fig. 3 showed that the B—O groups took part in the reaction network. However, the B—O groups themselves have no catalytic activity for C—H cleavage [17]. Extensive studies have showed that the B—OH groups easily generates from B—O species in the presence of steam [33,34]. Therefore, the high ODH activity in silicon boride catalyst most likely resulted from the B—OH groups formed from the "BO species" on the surfaces of silicon boride with an assistance of steam.

Further isotope-labeling measurements were used to investigate the reaction process. As shown in Fig. 5, when the silicon boride catalyst has been treated by D_2O (labeled as SiB-D) and then pulsed into C_3H_8 and O_2 at 535 °C, both HDO and D_2O were formed immediately with the formation of propylene, and their amounts gradually decreased during subsequent pulses. This result suggested that the H/D atoms in the SiB-D catalyst were abstracted during the reaction process, and also implied that the B—OH(D) groups of silicon boride catalyst might incorporate into the ODH reaction.

3.3. Kinetic analysis

Kinetic experiments were performed to gain insights into the reaction pathway of light alkanes ODH over the silicon boride catalyst. The effect of propane and oxygen concentrations on the reaction rate was shown in Fig. 4. Eq. (1) gave a rate expression for propane consumption,

$$r_{C3H8} = kP_{02}^{0.3}P_{C3H8}^{2.2} \quad (1)$$

k is the rate constant, P_{O2} and P_{C3H8} are partial pressure of O_2 and C_3H_8, respectively.

The kinetic analysis exhibited that the reaction order of oxygen approached 0.5. In our previous work [14], an ^{18}O isotope tracer study verified that an oxygen exchange between the surface oxygen atoms in the B—OH groups and molecular oxygen occurred in the reaction of ODH process at hydroxylated *h*-BN catalyst. Huang et al. [18] also found that the atomic exchange between $^{16}O_2$ and $^{18}O_2$ in the reaction of ODH process at *h*-BN catalyst. Therefore, it was reasonable to speculate that molecular oxygen may dissociate on surface of catalyst in the reaction process. As shown in Eq. (1), a near second-order dependence of propane concentration suggested that the activation of propane determined the total reaction rate. An increase in selectivity as increasing oxygen concentration (Fig. 4c) revealed that molecular oxygen favors the formation of propylene. Similar kinetic behaviors were also observed in ODH of ethane and isobutane (Fig. S9), which suggested that the light alkanes have an analogous reaction mechanism over silicon boride catalyst.

Moreover, the apparent activation energy (E_a, Fig. S10) were estimated to be 268 kJ mol^{-1}, 244 kJ mol^{-1} and 160 kJ mol^{-1} for ethane, propane and isobutane, respectively. The values of E_a were obvious higher than those reported for metal oxide catalysts. The difference in E_a of light alkanes does correspond to the difference in bond strength of the weakest C—H bond in each corresponding alkane (the order of the weakest C—H bond strength: C_2H_6 > C_3H_8 > i-C_4H_{10}), implying that the kinetically-relevant step might involve C—H cleavage during ODH using silicon boride catalyst.

4. Conclusions

We have shown that silicon boride is an active metal-free catalyst for oxidative dehydrogenation of light alkanes to valuable olefins with high selectivity. When the conversion of ethane, propane and isobutane reached 18.8%, 19.1% and 6.0%, the selectivity of total olefins were up to 98.0%, 94.4% and 96.4%, respectively. The light olefins productivity of 1.2–2.6 $g_{olefins}\ g_{cat}^{-1}h^{-1}$ were obtained. The antioxidant ability of silicon boride ensured the catalytic stability. Based on spectra and dynamics analysis, the B—OH groups generated from the "BO species" with the assistance of steam might be catalytic activity sites. This work experimentally supports that the catalytic origin of the boron species from the metal-free catalyst initiate the oxidative dehydrogenation of light alkanes.

Acknowledgements

This study was supported by state key program of National Natural Science Foundation of China (21733002), Joint Sino-German Research Project (21761132011), Cheung Kong Scholars Programme of China (T2015036).

Appendix A. Supplementary material

Supplementary data to this article can be found online at https://doi.org/10.1016/j.jcat.2018.11.014.

References

[1] S.R.G. Carrazán, C. Peres, J.P. Bernard, M. Ruwet, R. Ruiz, B. Delmon, Catalytic synergy in the oxidative dehydrogenation of propane over MgVO catalysts, J. Catal. 158 (1996) 452–476.

[2] M.A. De León, C. De Los Santos, L. Latrónica, A.M. Cesio, C. Volzone, J. Castiglioni, M. Sergio, High catalytic activity at low temperature in oxidative dehydrogenation of propane with Cr–Al pillared clay, Chem. Eng. J. 241 (2014) 336–343.

[3] Y.-M. Liu, Y. Cao, N. Yi, W.-L. Feng, W.-L. Dai, S.-R. Yan, H.-Y. He, K.-N. Fan, Vanadium oxide supported on mesoporous SBA-15 as highly selective catalysts in the oxidative dehydrogenation of propane, J. Catal. 224 (2004) 417–428.

[4] C.A. Gartner, A.C. van Veen, J.A. Lercher, Oxidative dehydrogenation of ethane: common principles and mechanistic aspects, ChemCatChem 5 (2013) 3196–3217.

[5] G. Liu, L. Zeng, Z.-J. Zhao, H. Tian, T. Wu, J. Gong, Platinum-modified ZnO/Al2O3 for propane dehydrogenation: minimized platinum usage and improved catalytic stability, ACS Catal. 6 (2016) 2158–2162.

[6] Z.J. Zhao, C.C. Chiu, J. Gong, Molecular understandings on the activation of light hydrocarbons over heterogeneous catalysts, Chem. Sci. 6 (2015) 4403–4425.

[7] Z.J. Zhao, T. Wu, C. Xiong, G. Sun, R. Mu, L. Zeng, J. Gong, Hydroxyl-mediated non-oxidative propane dehydrogenation over VOx/gamma-Al2 O3 catalysts with improved stability, Angew. Chem. 57 (2018) 6791–6795.

[8] L. Leveles, K. Seshan, J. Lercher, L. Lefferts, Oxidative conversion of propane over lithium-promoted magnesia catalyst: I. Kinetics and mechanism, J. Catal. 218 (2003) 296–306.

[9] R.B. Watson, U.S. Ozkan, K/Mo catalysts supported over sol-gel silica–titania mixed oxides in the oxidative dehydrogenation of propane, J. Catal. 191 (2000) 12–29.

[10] A. Bodke, D. Olschki, L. Schmidt, E. Ranzi, High selectivities to ethylene by partial oxidation of ethane, Science 285 (1999) 712–715.

[11] T. Hantke, I. Zimmermann, An approximative method for the evaluation of the partial heats of fusion of the once folded and extended modification of poly (ethylene oxide) 6000, Thermochim Acta 345 (2000) 67–72.

[12] L. Shi, Y. Wang, B. Yan, W. Song, D. Shao, A.H. Lu, Progress in selective oxidative dehydrogenation of light alkanes to olefins promoted by boron nitride catalysts, Chem. Commun. 54 (2018) 10936–10946.

[13] J.T. Grant, C.A. Carrero, F. Goeltl, J. Venegas, P. Mueller, S.P. Burt, S.E. Specht, W. P. McDermott, A. Chieregato, I. Hermans, Selective oxidative dehydrogenation of propane to propene using boron nitride catalysts, Science 354 (2016) 1570–1573.

[14] L. Shi, D. Wang, W. Song, D. Shao, W.-P. Zhang, A.-H. Lu, Edge-hydroxylated boron nitride for oxidative dehydrogenation of propane to propylene, ChemCatChem 9 (2017) 1788–1793.

[15] L. Shi, B. Yan, D. Shao, F. Jiang, D. Wang, A.-H. Lu, Selective oxidative dehydrogenation of ethane to ethylene over a hydroxylated boron nitride catalyst, Chin. J. Catal. 38 (2017) 389–395.

[16] J.T. Grant, W.P. McDermott, J.M. Venegas, S.P. Burt, J. Micka, S.P. Phivilay, C.A. Carrero, I. Hermans, Boron and boron-containing catalysts for the oxidative dehydrogenation of propane, ChemCatChem 9 (2017) 3623–3626.

[17] L. Shi, D. Wang, A.-H. Lu, A viewpoint on catalytic origin of boron nitride in oxidative dehydrogenation of light alkanes, Chin. J. Catal. 39 (2018) 908–913.

[18] R. Huang, B. Zhang, J. Wang, K.-H. Wu, W. Shi, Y. Zhang, Y. Liu, A. Zheng, R. Schlögl, D.S. Su, Direct insight into ethane oxidative dehydrogenation over boron nitrides, ChemCatChem 9 (2017) 3293–3297.

[19] Y. Wang, L. Zhao, L. Shi, J. Sheng, W. Zhang, X.-M. Cao, P. Hu, A.-H. Lu, Methane activation over a boron nitride catalyst driven by in situ formed molecular water, Catal. Sci. Technol. 8 (2018) 2051–2055.

[20] F. Guo, P. Yang, Z. Pan, X.N. Cao, Z. Xie, X. Wang, Carbon-doped BN nanosheets for the oxidative dehydrogenation of ethylbenzene, Angew. Chem. 56 (2017) 8231–8235.

[21] B. Frank, M. Morassutto, R. Schomäcker, R. Schlögl, D.S. Su, Oxidative dehydrogenation of ethane over multiwalled carbon nanotubes, ChemCatChem 2 (2010) 644–648.

[22] X. Lin, K.R. Poeppelmeier, E. Weitz, Oxidative dehydrogenation of ethane with oxygen catalyzed by K-Y zeolite supported first-row transition metals, Appl. Catal. A 381 (2010) 114–120.

[23] B. Solsona, T. Blasco, J.M. López Nieto, M.L. Peña, F. Rey, A. Vidal-Moya, Vanadium oxide supported on mesoporous MCM-41 as selective catalysts in the oxidative dehydrogenation of alkanes, J. Catal. 203 (2001) 443–452.

[24] Z.-J. Sui, J.-H. Zhou, Y.-C. Dai, W.-K. Yuan, Oxidative dehydrogenation of propane over catalysts based on carbon nanofibers, Catal. Today 106 (2005) 90–94.

[25] B. Frank, J. Zhang, R. Blume, R. Schlogl, D.S. Su, Heteroatoms increase the selectivity in oxidative dehydrogenation reactions on nanocarbons, Angew. Chem. 48 (2009) 6913–6917.

[26] I. Gniot, P. Kirszensztejn, M. Kozłowski, Oxidative dehydrogenation of isobutane using modified activated carbons as catalysts, Appl. Catal. A 362 (2009) 67–74.

[27] J. de Jesús Díaz, L.M.C. Velásquez, J.L. Figueiredo Suárez, Oxidative dehydrogenation of isobutane over activated carbon catalysts, Appl. Catal. A 311 (2006) 51–57.

[28] Y. Zhou, J. Lin, L. Li, X. Pan, X. Sun, X. Wang, Enhanced performance of boron nitride catalysts with induction period for the oxidative dehydrogenation of ethane to ethylene, J. Catal. 365 (2018) 14–23.

[29] W.E. Moddeman, A.R. Burke, W.C. Bowling, D.S. Foose, Surface oxides of boron and B12O2 as determined by XPS, Surf. Interface Anal. 14 (1989) 224–232.

[30] L.M. Litz, R.A. Mercuri, Oxidation of boron carbide by air water, and air-water mixtures at elevated temperatures, J. Electrochem. Soc. 111 (1963) 921–925.

[31] G. Liu, Z.J. Zhao, T.F. Wu, L. Zeng, J.L. Gong, Nature of the active sites of VOx/Al2O3 catalysts for propane dehydrogenation, ACS Catal. 6 (2016) 5207–5214.

[32] C. Gautam, A.K. Yadav, A.K. Singh, A review on infrared spectroscopy of borate glasses with effects of different additives, ISRN Ceram. 2012 (2012) 1–17.

[33] J.L. Parsons, M.E. Milberg, Vibrational spectra of vitreous B2o3.Xh2o, J. Am. Ceram. Soc. 43 (1960) 326–330.

[34] O.M. Moon, B.C. Kang, S.B. Lee, J.H. Boo, Temperature effect on structural properties of boron oxide thin films deposited by MOCVD method, Thin Solid Films 464–465 (2004) 164–169.